

Influence of syngas composition on the transient behavior of a Fischer–Tropsch continuous slurry reactor

M. Bremaud^a, P. Fongarland^{a,*}, J. Anfray^{a,b}, S. Jallais^c,
D. Schweich^b, A.Y. Khodakov^a

^a *Laboratoire de Catalyse de Lille, USTL, Bâtiment C3, 59655 Villeneuve d'Ascq, France*

^b *Laboratoire de Génie des Procédés Catalytiques, 43 Bd du 11 novembre 1918, BP 2077, 69616 Villeurbanne Cedex, France*

^c *AIR LIQUIDE, CRCD, 78354 Jouy-en-Josas, France*

Abstract

The influence of syngas composition on the initial behaviour of a Co/Al₂O₃ catalyst in Fischer–Tropsch reaction has been studied in a continuous perfectly mixed slurry reactor for an inlet H₂/CO ratio between 1.6 and 3.35 keeping other conditions constant ($T = 220\text{ }^{\circ}\text{C}$, $P = 2\text{ MPa}$). Significantly different behaviors of initial deactivation for CO conversion have been observed with different H₂/CO ratios. It was observed that the deactivation increases with increase in H₂/CO ratio and in carbon monoxide conversion. The computed liquid concentrations of CO, H₂ and H₂O have shown that water is the most abundant species in the liquid phase of the reactor during our experiments. The concentration of the water produced by the FT reaction seems to be the key parameter responsible of the initial behavior and then of the initial deactivation. For moderate levels of water ($C_{\text{H}_2\text{O}}^{\text{L}}/C_{\text{H}_2}^{\text{L}} < 4$ corresponding to $P_{\text{H}_2\text{O}}/P_{\text{H}_2} < 0.4$), a simple kinetic model assuming a reversible oxidation of cobalt active sites by water in competition with their reduction by hydrogen seems to represent satisfactorily the initial behaviour of the catalyst. For higher water concentrations, the irreversible deactivation should be probably taken into consideration.

© 2005 Elsevier B.V. All rights reserved.

Keywords: Syngas; Fischer–Tropsch; Slurry

1. Introduction

Growing demand for clean fuels has inspired development of new technologies for the conversion of abundant natural gas reserves to liquid hydrocarbons. Synthetic fuels produced via Fischer–Tropsch (FT) synthesis contain lower concentrations of sulfur and can be tailored for specific industry applications. Both fixed-bed and slurry reactors are commonly used to perform FT reaction. Principal advantages of the slurry reactor are a better temperature control, absence of intraparticle mass transfer limitations and a possibility to recycle the catalyst. To simulate this complex unit, both reactor hydrodynamics and reaction kinetics need to be modeled. Previous studies have reported considerable evolution of FT activity and hydrocarbon selectivities during the reactor start-up for iron [1] or cobalt catalysts [2,3]. This

evolution is traditionally attributed to catalyst deactivation but few studies are reporting models to describe this complex behavior [2,4]. Water is a major product of FT synthesis. Several previous reports have shown the effect of water added into the feed on the catalytic performance of cobalt catalysts. Very few of them, however, have addressed the effect of water produced by the reaction itself. An attempt was made in the present work to propose a simplified model based on the experimental measurements and calculated liquid concentrations to describe this initial transient behavior of the catalytic system in a slurry continuous stirred tank reactor.

2. Experimental

The transient behavior of FT reaction over a commercial catalyst Co/Al₂O₃ has been studied in a 300 mL continuous stirred tank reactor (CSTR) from Autoclave Engineers. The reactor is equipped with a 6-blades radial impeller and

* Corresponding author.

E-mail address: pascal.fongarland@univ-lille1.fr (P. Fongarland).

assumed to be perfectly mixed. The macromixing of the solid particles has been qualitatively examined at ambient conditions with a transparent tank and *n*-C₁₄ hydrocarbon as a liquid, which has a density close to the FT wax under our FT reaction conditions (220 °C and 2 MPa). This preliminary study confirmed that the solid phase is completely suspended in the liquid at 1500 rpm for a concentration of solids up to 30% (w/w). The experimental set-up is presented in the Fig. 1. The reactor (2) is fed with syngas through the mass flow controllers (1). The syngas is then introduced inside the reactor by a sparger placed at the bottom of the tank. The volume of gas–liquid–solid emulsion ($V_{\text{overall}} \approx 70$ mL) is self-controlled by overflow through an immersed 10 μm filter. The outlet stream is separated in a hot condenser (4) (150 °C, 2 MPa) followed by a cold one (5) (10 °C, 2 MPa). The gas flow is depressurized to the ambient pressure (6), sent either to an online gas chromatograph (8) or to a volumetric gas flow-meter (7). The catalyst is a commercial Co/Al₂O₃ with 15% of Co (w/w) and 50 μm mean particle diameter. It is reduced inside the reactor by hydrogen at atmospheric pressure (GHSV = $1.83 \text{ N m}^3 \text{ s}^{-1} \text{ kg}_{\text{cat}}^{-1}$) at 400 °C (ramp rate: $2 \text{ }^\circ\text{C min}^{-1}$, dwell at 400 °C for 8 h). The initial wax (Shell SX70) is then added to the catalyst under inert atmosphere. A second reduction procedure has involved an ex situ fixed-bed hydrogen pretreatment with the same temperature program. Our data show that both reduction procedures lead to similar catalytic behavior of the cobalt catalyst.

After the reduction step, the syngas is introduced at a desired flowrate. The temperature of the reactor is then increased to 220 °C at a rate of $2 \text{ }^\circ\text{C min}^{-1}$. The gas effluent is analyzed by a gas chromatograph (Varian 3800) equipped with a TCD detector to quantify CO, CH₄, N₂, CO₂ or H₂ (He or Ar carrier gas, molecular sieve 13X column) and a FID detector for paraffins and olefins from C₁ to C₉ (He carrier gas, capillary column Chrompack CP-Plot). Wax and a mixture of diesel and aqueous products are periodically withdrawn from the hot and cold condensers, respectively. Different inlet H₂/CO ratios have been tested covering a range from 1.6 to 3.35 at a constant temperature (220 °C), total pressure (2 MPa) and inlet GHSV ($3.55 \times 10^{-4} \text{ N m}^3 \text{ s}^{-1} \text{ kg}_{\text{cat}}^{-1}$) for all experiments.

3. Liquid phase composition calculation

The reconstruction of the liquid phase composition under the FT reaction conditions (220 °C and 2 MPa) has been obtained by flash calculation to obtain equality of the computed gas and liquid fugacities. For the gas phase, the Peng–Robinson equation of state has been chosen to compute the gas phase fugacity of each component. Concerning the liquid phase, the mole fraction has been computed with the Henri's law for supercritical components such as CO, H₂, H₂O or light hydrocarbons and with an activity model for heavier

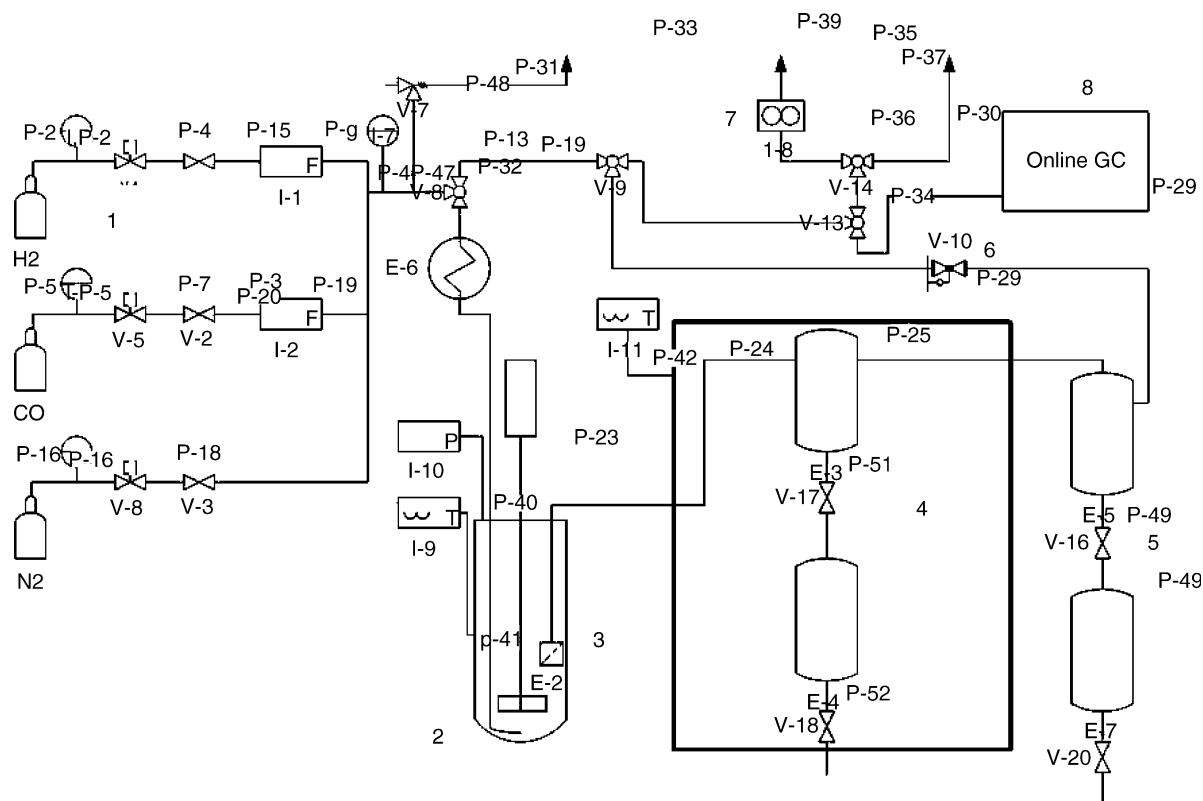


Fig. 1. Simplified scheme of the experimental set-up used in this study (1: syngas feeding, 2: reactor, 3: filter, 4: hot condenser, 5: cold condenser, 6: Grove valve, 7: volumetric gas flowrate meter, 8: online gas-chromatography).

Table 1
Summary of the experimental runs and quasi steady-state results

	Inlet H ₂ /CO (molar ratio)	CO conversion %	CH ₄ selectivity %	R_{CO} (mol s ⁻¹ kg _{cat} ⁻¹)	Outlet liquid C_{H_2}/C_{CO}^c	Steady-state regime (days)
RUN01 ^a	1.6	19.2	12.6	1.14×10^{-3}	1.14	9
RUN02 ^a	2.1	32.3	13.5	1.61×10^{-3}	1.34	13
RUN03 ^a	3.35	61.8	27.8	2.22×10^{-3}	4.17	22
RUN04 ^b	2.1	27.4	17.9	1.37×10^{-3}	1.55	5

Reactor start-up conditions.

^a Wax SX70.

^b RUN 01.

^c Computed at 220 °C and 2 MPa.

hydrocarbons. Both of these parameters have been calculated from the Marano and Holder asymptotic correlations [5]. Finally, the concentrations C_i^L of CO, H₂ and H₂O in the liquid phase of the reactor are obtained from the following relation: $C_i^L = x_i/v_m^L$ where x_i is the liquid mole fraction of i and v_m^L is the liquid molar volume.

4. Results and discussion

Preliminary experiments have been performed to measure the volumetric gas–liquid mass transfer coefficients $k_L a$ and solubilities of H₂ at the temperature and pressure of the reaction to compare with the values predicted by the thermodynamic model. Invariance of CO conversion for impeller rate beyond 500 rpm coupled with the experimental $k_L a$ for H₂ in the initial wax SX70 confirmed the absence of external mass transfer limitations. Values of computed Weisz modulus are lower than 10^{-3} indicating the absence of intraparticle mass transfer limitations and the regime of chemical kinetics.

4.1. Steady-state

The total length of each run was between 11 and 25 days depending on the experimental conditions. The length of the run is related to the time necessary to reach the steady-state regime where the CO conversion and hydrocarbon composition at the reactor outlet have been stabilized. At the steady-state regime, as it was previously predicted [1], higher CO conversions and CH₄ selectivities have been observed at higher H₂/CO ratios (see Table 1). For H₂/CO equal to 1.6 (RUN 01), CO conversion and CH₄ selectivity are 19 and 13%, respectively, while for a large H₂/CO ratio (3.35) they are between 62 and 28%, respectively. An intermediate CO conversion and CH₄ selectivity is obtained for the inlet H₂/CO equal to 2.1 (RUN 03). The rate of CO consumption R_{CO} is calculated from the mass balance over the reactor neglecting the accumulation term since we are assuming the steady-state regime:

$$R_{CO} = \frac{F_{CO}^{in} - F_{CO}^{ex}}{W}$$

where F_{CO} is the CO molar flowrate at the inlet or outlet of the reactor and W is the mass of catalyst. For the RUN01 to

the RUN03, R_{CO} is found to lay between 1.14×10^{-3} and 2.22×10^{-3} mol s⁻¹ kg_{cat}⁻¹. It increases with the inlet H₂/CO molar ratio. The computed outlet liquid concentration ratio C_{H_2}/C_{CO} from flash calculations increases as well with the inlet ratio H₂/CO.

RUN04 was performed next to end of RUN01 (25 days). It starts with the (aged) catalyst sample of RUN01 and the wax in the reactor produced during this run. Then the H₂/CO inlet ratio was switched from 1.6 to 2.2. Temporal evolution of CO conversion for RUN02 and RUN04 (Fig. 3) suggests that the steady-state regime for the RUN02 is not completely attained, contrary to the apparent stabilization of CO conversion observed in Fig. 2 (see also Fig. 3).

4.2. Initial transient behavior

Fig. 2 shows that the evolution of CO conversion with time strongly depends on the H₂/CO ratio. At low H₂/CO (corresponding to low conversion, RUN01), CO conversion is first decreasing and attains rapidly a plateau in 2 days (see Fig. 2). In this case, it is not likely that the initial decrease in conversion could be attributed to the deactivation. During the first day, the effect of the reactor hydrodynamics for the

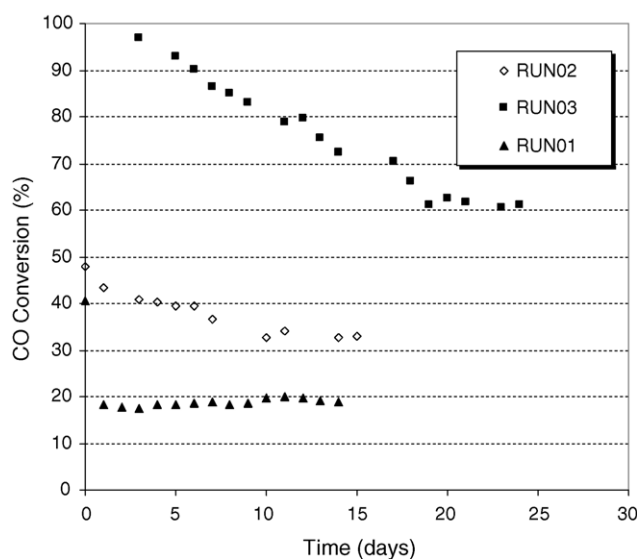


Fig. 2. Temporal evolution of the CO conversion for the RUN01 to RUN03 ($T = 220$ °C, $P = 2$ MPa, initial wax SX70, $1.6 < \text{inlet H}_2/\text{CO} < 3.2$).

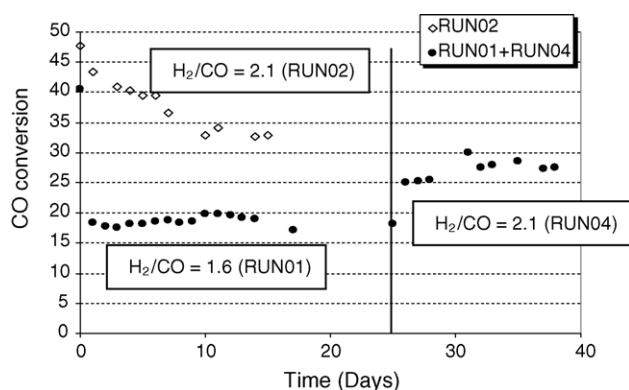


Fig. 3. Evolution of CO conversion with time for the RUN01, RUN02 and RUN04.

gas phase is expected to be rather important due to the backmixing of the stirred tank reactor. When the inlet H_2/CO is higher, the initial behavior of the catalyst is completely different. A slow but gradual decrease in CO conversion is then observed (RUN02 and RUN03).

For $H_2/CO = 2.1$, Pinna et al. [3] reported a similar transient behavior using a 15% w/w Co/Al_2O_3 catalyst in a slurry reactor. A gradual decrease in the CO conversion from 45 to 35% in 19 days was reported. These authors attributed the slow drift of selectivity toward heavy HC to the renewal of the initial wax. Conversely, the initial transient of CO conversion is more difficult to explain.

Let us consider several phenomena which could be involved in the progressive decrease in carbon monoxide conversion during reactor start-up. The change in conversion reflects a change in the reaction rate. The latter can be due to a change in the liquid phase composition with respect to the reactant (CO and H_2) and potentially inhibiting products (H_2O). This change can in turn be due to a modification of the gaseous species solubility owing to the wax composition drift [6,7]. However, vapor–liquid equilibrium computations showed only a slight evolution of these solubilities. The computed Henry's constants (defined here by the relation $H_i = \frac{P_i}{x_i}$ with P_i the partial pressure of i and x_i is the liquid mole fraction of i) for all runs (RUN01 to RUN04) are varying from 42 to 46 MPa for H_2 , between 33 and 36 MPa for CO and between 4 and 5 MPa for H_2O . These small variations cannot explain for the decrease in CO conversion.

Catalyst coking may also be responsible for the observed decrease in the FT rate. Coking is generally attributed to unsaturated precursors, such as olefins. However, olefin production is depleted when high H_2/CO ratios are used. This should induce less deactivation, whereas the reverse is observed.

Sintering of the metallic particles dispersed on the alumina support may also cause the apparent deactivation. As explained above, RUN04 replicates the conditions of RUN02 (fresh catalyst) with an aged catalyst (of RUN01). If sintering due to time on stream condition were prevailing, CO conversion should be smaller in RUN04 than in RUN02.

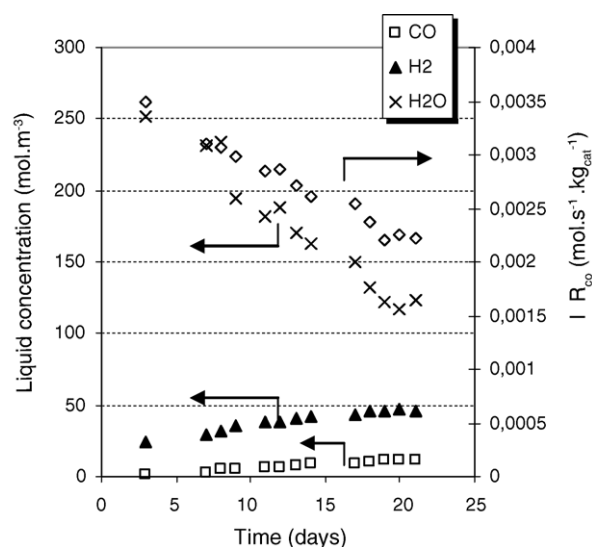


Fig. 4. Evolution of liquid phase concentration of CO, H_2 , H_2O and R_{CO} for the RUN03 (inlet $H_2/CO = 3.35$).

Fig. 3 and Table 1 show that there is no significant difference. Note that during the initial part of RUN04 the catalyst did not exhibit any deactivation (Fig. 3), whereas a significant deactivation was observed in RUN02.

Water is a product of FT reaction and its production rate is proportional to the CO conversion (Fig. 4; Table 2). Thus, the water oxidation mechanism proposed by several authors [2,8–12] could possibly explain the different initial behavior of the catalyst, though thermodynamics does not predict the formation of oxides from bulk metallic phase under FT conditions [8]. With a Pt promoted Co/Al_2O_3 , Li et al. observed a quick reversible decrease of the CO conversion after each point wise additions of water into the reactor (210 °C, 2.9 MPa in a CSTR, water volume added <25%). This decrease was irreversible for higher water concentration. Catalyst characterization suggested no modification of the catalyst structure at low water pressures, while transformation of metallic cobalt into aluminates at higher water levels has been advanced to explain the irreversible deactivation [12]. Concerning the reversible deactivation at low water pressures, Li et al. [2] suggested that the amount of active sites available for FT reaction depends on the partial pressures of water (oxidation–deactivation of the active sites *) and hydrogen (reduction of the oxidized sites $^*-O$). This mechanism may be simply represented by:



Table 2
Minimum and maximum values of the computed $C_{H_2O}^L/C_{H_2}^L$ and the corresponding P_{H_2O}/P_{H_2} for all the experiments

	$C_{H_2O}^L/C_{H_2}^L$	P_{H_2O}/P_{H_2}
RUN01	1–2.9	0.13–0.15
RUN02	2–4	0.22–0.43
RUN03	2.5–10	0.27–1.15
RUN04	1.6	0.17

Since water is produced by the FT reaction, the decrease in the CO conversion observed in the RUN02 and RUN03 may be interpreted in terms of the decrease in the number of active sites due to the cobalt oxidation by water. It can be suggested that the higher is the concentration of the produced water in the liquid medium, the more significant the deactivation is. Fig. 4 presents the evolution of CO, H₂, H₂O concentrations and CO conversion for the RUN03. This run exhibits the strongest deactivation. Table 2 shows that at FT conditions, the water concentration in the liquid phase is much higher than that of hydrogen even at low conversions (RUN01).

The boundary between irreversible and reversible deactivation by water has been found by Li et al. [2] at $P_{\text{H}_2\text{O}}/P_{\text{H}_2}$ around 0.6. This suggests that RUN01, RUN02 and RUN04 show the reversible deactivation by water discussed by Li et al. [2]. On the other hand, irreversible deactivation proceeds during RUN03. The following simple model can be proposed to describe the reversible deactivation. Assuming the total number of sites (reduced and oxidized) to remain constant during the run and that Eq. (1) is a pseudo-elementary step, the mass balance for the active sites yields the following expression:

$$-\frac{d[*]}{dt} = k_d[*]C_{\text{H}_2\text{O}}^L - k_r(1 - [*])C_{\text{H}_2}^L \quad (2)$$

$$R_{\text{CO}} = R_{\text{CO}}^0[*] = [*] \times \frac{aC_{\text{CO}}^L C_{\text{H}_2}^L}{(1 + bC_{\text{CO}}^L)^2} \quad (3)$$

In these expressions (Eqs. (2) and (3)), $[*]$ is the fraction of catalytic sites available for FT synthesis (not the fraction of “free” catalytic sites), i.e., the “deactivation function” as defined by Froment and Bischoff [13]. R_{CO}^0 is the reaction rate in the absence of deactivation and the expression has been taken from standard kinetic analyses at steady-state [6].

The concentrations of CO, H₂ and H₂O in the liquid phase have been obtained for each experimental CO conversion. Kinetic parameters (Table 3) have been fitted by minimizing the square sum of the differences between experimental and calculated R_{CO} with the transient data of RUN02 and steady-state experimental points of RUN04. The deactivation constant k_d as expected is very low compared to the FT kinetic constant a . Modelling deactivation kinetics for RUN03 using the set of kinetic parameters of RUN02 does not lead to satisfactory results. This supports the possible irreversible deactivation process that requires a more

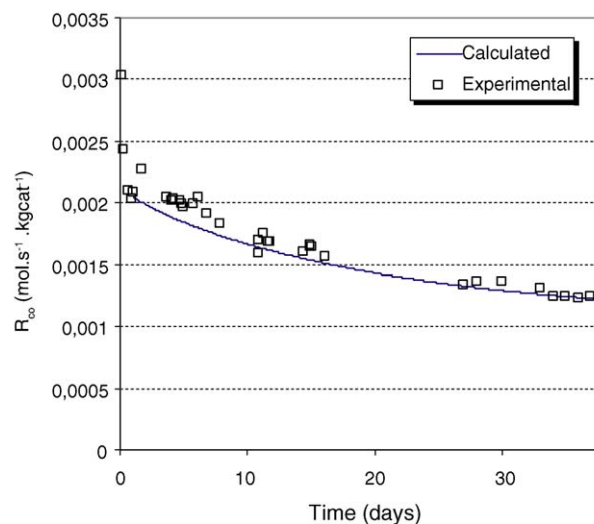


Fig. 5. Calculated and experimental rate of CO as a function of time for RUN02 with steady-state RUN04 experimental points (after 28 days).

sophisticated model than that proposed for the moderate water concentrations.

5. Conclusion

The influence of syngas composition on the initial behaviour of a Co/Al₂O₃ catalyst in FT reaction has been studied in a continuous perfectly mixed slurry reactor. When using freshly activated catalyst, it was found that at carbon monoxide conversion higher than 30% the FT reaction rate is gradually decreasing with time, while no deactivation was observed at low carbon monoxide conversion. The deactivation is probably due to reoxidation of cobalt particles by water. At moderate water levels ($P_{\text{H}_2\text{O}}/P_{\text{H}_2} = 0.22 - 0.43$), the catalyst deactivation may be represented by a simple kinetic model assuming a reversible catalyst oxidation by water and reduction by hydrogen. This approach is not appropriate for the higher water concentrations due to a probable irreversible catalyst deactivation at these conditions (Fig. 5).

Acknowledgement

Authors would like to thank the Air Liquide company for their financial support.

References

- [1] H. Schulz, G. Schaub, M. Claeys, T. Riedel, Appl. Catal. A 186 (1999) 215.
- [2] J. Li, X. Zhan, Y. Zhang, G. Jacobs, T. Das, B.H. Davis, Appl. Catal. A 228 (2002) 203.
- [3] D. Pinna, E. Tronconi, L. Lietti, R. Zennaro, P. Forzatti, J. Catal. 214 (2003) 251.

Table 3
Kinetic parameters obtained for RUN02 and RUN04

	Kinetic parameters
k_d	$3.39 \times 10^{-9} \text{ m}^3 \text{ s}^{-1} \text{ mol}^{-1}$
k_r	$1.46 \times 10^{-9} \text{ m}^3 \text{ s}^{-1} \text{ mol}^{-1}$
a	$7.16 \times 10^3 \text{ m}^3 \text{ s}^{-1} \text{ mol}^{-1} \text{ kg}_{\text{cat}}^{-1}$
b	$1.97 \times 10^3 \text{ m}^3 \text{ mol}^{-1}$

- [4] Q. Qin, D. Ramkrishna, *Ind. Eng. Chem. Res.* 43 (2004) 2912.
- [5] J.J. Marano, G.D. Holder, *Fluid Phase Equilib.* 138 (1997) 1.
- [6] I.C. Yates, C.N. Satterfield, *Energy Fuels* 5 (1991) 168.
- [7] E. van Steen, H. Schulz, *Appl. Catal. A* 186 (1999) 309.
- [8] P.J. van Berge, J. van de Loosdrecht, S. Barradas, A.M. van der Kraan, *Catal. Today* 58 (2000) 321.
- [9] M.W.J. Crajé, A.M. van der Kraan, J. van de Loosdrecht, P.J. van Berge, *Catal. Today* 71 (2002) 369.
- [10] M. Rothaemel, K.F. Hanssen, A. Edd Blekkan, D. Schanke, A. Holmen, *Catal. Today* 38 (1997) 79.
- [11] A.M. Hilmen, D. Schanke, K.F. Hanssen, A. Holmen, *Appl. Catal. A: Gen.* 186 (1999) 169.
- [12] G. Jacobs, T.K. Das, P.M. Patterson, J. Li, L. Sanchez, B.H. Davis, *Appl. Catal. A* 247 (2003) 335.
- [13] G.F. Froment, K.B. Bischoff, *Chemical Reactor Analysis and Design*, John Wiley and Sons Ltd., 1990.